Dalton Transactions

PAPER

View Article Online
View Journal | View Issue

Cite this: *Dalton Trans.*, 2018, **47**, 12901

Carbonate: an alternative dopant to stabilize new perovskite phases; synthesis and structure of $Ba_3Yb_2O_5CO_3$ and related isostructural phases $Ba_3Ln_2O_5CO_3$ (Ln = Y, Dy, Ho, Er, Tm and Lu)†

Joshua Deakin,[a] Ivan Trussov,[a] Alexandra Gibbs,[b] Emma Kendrick[c] and Peter R. Slater *[a]

Received 2nd July 2018,
Accepted 10th August 2018

DOI: 10.1039/c8dt02691b

rsc.li/dalton

In this paper we report the synthesis of the new layered perovskite oxide carbonate, $Ba_3Yb_2O_5CO_3$. This phase is formed when $3BaCO_3 : 1Yb_2O_3$ mixtures are heated in air at temperatures ≤1000 °C, while above this temperature the carbonate is lost and the simple oxide phase $Ba_3Yb_4O_9$ is observed. The structure of $Ba_3Yb_2O_5CO_3$ was determined from neutron diffraction studies and consists of a tripled perovskite with double Yb–O layers separated by carbonate layers, the first example of a material with such a structure. Further studies showed that analogous $Ba_3Ln_2O_5CO_3$ phases could be formed for other rare earths (Ln = Y, Dy, Ho, Er, Tm and Lu). The results highlight the ability of the perovskite structure to accommodate carbonate groups, and emphasise the need to consider their potential presence particularly for perovskite systems prepared in lower temperature synthesis routes.

Introduction

Perovskite materials have attracted considerable interest due to a wide range of technologically important properties displayed by materials with this structure-type, including superconductivity, ionic conductivity, colossal magnetoresistance, ferroelectric properties, and the ability to catalyse a range of reactions. In addition to this rich wealth of properties, perovskites also display a wealth of interesting and, at time, unexpected structural diversity. In particular, research on high T_c cuprate superconductors showed the ability of the perovskite structure to accommodate carbonate and other oxyanions (borate, nitrate, sulfate, phosphate).[1–12] In these situations, the C, B, N, P, S of the oxyanion group resides on the perovskite B cation site, while the oxide ions of this group fill 3 (C, B, N)–4 (P, S) of the available 6 oxide ion positions around this site, albeit displaced so as to achieve the required geometry for the oxyanion. The incorporation of oxyanions into other perovskite transition metal containing systems has also subsequently been reported, *e.g.* $Sr(Co/Fe/Mn)O_{3-\delta}$, $La_{1-x}Sr_xCo_{0.8}Fe_{0.2}O_{3-\delta}$, $Ba_{1-x}Sr_xCo_{0.8}Fe_{0.2}O_{3-\delta}$, $CaMnO_3$ and $La_{1-x}Sr_xMnO_3$-type materials.[13–30] Recently the incorporation of sulfate and phosphate have also been reported in $Ba_2(In/Sc)_2O_5$ leading to new cubic perovskites with high oxide ion conductivity/proton conductivity.[31–33]

In terms of these doping studies, it has been shown that oxyanions such as sulfate, borate, and phosphate exhibit higher thermal stability in the structure than carbonate. Therefore, work on incorporating carbonate has commonly employed reaction in evacuated quartz tubes to achieve reaction while preventing carbonate loss.[15–19] As such, other researchers may be viewing such carbonate containing systems as "exotic" compounds, which would not be formed under conventional synthesis conditions. This is a particularly worrying omission, since there is a growing trend in research to move to lower temperature synthesis (*e.g.* sol gel) routes where carbonate may be present. Indeed evidence for the importance of carbonate in materials is illustrated by recent work on other structure types; for example Li *et al*. have shown that hexagonal "$YAlO_3$" is an oxide carbonate,[34] with a true composition of $Y_3Al_3O_8CO_3$, while orthorhombic Ba_2TiO_4 has also been recently shown to contain carbonate.[35]

While prior carbonate doped perovskite work has focused on systems containing transition metals, such as Cu, here we extend such studies to investigate whether a perovskite phase could be formed for non-transition metal systems, with synthesis in air rather than evacuated quartz tubes. In particular, given that a cubic perovskite, $Ba_2Yb_{1.5}P_{0.5}O_{5.5}$ has been

[a]*School of Chemistry, University of Birmingham, Birmingham, B15 2TT, UK. E-mail: p.r.slater@bham.ac.uk; Fax: +44(0) 1214 144403; Tel: +44(0) 1214 148906*
[b]*ISIS Facility, Rutherford Appleton Laboratory, Harwell Oxford, Didcot, OX11 0QX, UK*
[c]*Warwick Manufacturing Group, University of Warwick, Coventry, CV4 7AL, UK*

†Electronic supplementary information (ESI) available. See DOI: 10.1039/c8dt02691b

recently shown to be stabilised by phosphate incorporation, we therefore investigated the possibility that a perovskite containing carbonate could be formed in the $BaCO_3$: Yb_2O_3 phase diagram at lower temperatures (≤1000 °C) to allow carbonate incorporation. This led to the identification of a new phase with $BaCO_3$: Yb_2O_3 ratio of 3 : 1, and in this paper we report the synthesis and structural characterisation of this new carbonate containing perovskite system. In addition, in order to investigate the versatility for carbonate incorporation in perovskites, we also illustrate the formation of isostructural phases for a range of other rare earths.

Experimental

High purity $BaCO_3$, Yb_2O_3 were used to prepare $Ba_3Yb_2O_5CO_3$. The powders were intimately ground in a 3 : 1 $BaCO_3$, Yb_2O_3 ratio and heated initially to 900 °C for 12 h in air. They were then reground and reheated to 1000 °C in air for a further 24 h with regrinding every 12 hours. After the initial synthesis in air, we also investigated the formation of this compound under dry N_2 in order to allow higher temperature heat treatment by reducing CO_2 loss through reaction with moisture in the air. In this case, it was found that $Ba_3Yb_2O_5CO_3$ could be prepared in a shorter timescale (12 h) by employing a higher temperature (1050 °C). Note heat treatment in air at 1050 °C leads to large $Ba_3Yb_4O_9$ impurities due to carbonate loss. These synthesis routes were then used to make a wider range of isostructural $Ba_3Ln_2O_5CO_3$ systems (Ln = Y, Dy, Ho, Er, Tm and Lu).

Phase identification and initial structure determination was carried out by Rietveld profile refinement using powder X-ray diffraction data (XRD) collected on a Panalytical Empyrean diffractometer (Cu Kα radiation) or a Bruker D2 diffractometer (Co Kα radiation).

Raman data for $Ba_3Yb_2O_5CO_3$ were collected on a Renishaw inVia Raman microscope using a 532 nm laser in order to confirm the presence of carbonate in the material.

For the detailed structure determination on $Ba_3Yb_2O_5CO_3$, time of flight powder neutron diffraction (NPD) data were recorded on the HRPD diffractometer at the ISIS pulsed spallation source (Rutherford Appleton Laboratory, UK). Structure refinements using the NPD data were performed using the Rietveld method with the General Structure Analysis System GSAS-II suite of programs.[36]

Results and discussion

Phase identification and structure determination of $Ba_3Yb_2O_5CO_3$

Initially a range of $BaCO_3$: Yb_2O_3 mixtures with different ratios were investigated, and it was found that a new phase was observed with an optimum $BaCO_3$: Yb_2O_3 ratio of 3 : 1. The formation of this phase was shown to be very sensitive to the synthesis temperature (Fig. 1). At temperatures up to 900 °C, no reaction was observed, and the XRD pattern showed simply the presence of the starting materials, $BaCO_3$ and Yb_2O_3. Heating to 950 °C led to the appearance of the new perovskite phase, with the purity improving by heating at 1000 °C. At temperatures above 1000 °C, this compound was shown to decompose, and the formation of the simple oxide $Ba_3Yb_4O_9$ was observed, which suggested that the initial perovskite phase contained carbonate.

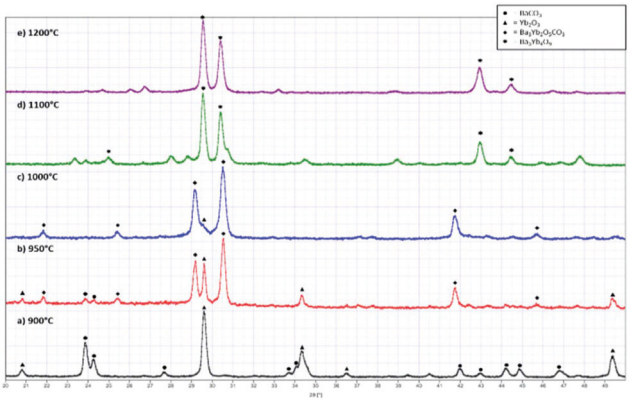

Fig. 1 X-ray diffraction patterns for a 3 : 1 mixture of $BaCO_3$: Yb_2O_3 heated at different temperatures, showing the formation of a new layered perovskite phase, $Ba_3Yb_2O_5CO_3$ between 950–1000 °C, with decomposition of this phase to give $Ba_3Yb_4O_9$ at higher temperatures.

Indexing the pattern for this new phase gave a tetragonal perovskite-related cell which was tripled along the *c* direction. From the unit cell parameters obtained, a structure was then surmised based on the assumption that oxygen vacancies around the Yb sites would be less favourable. This predicted structure consisted of double Yb–O layers separated by carbonate layers.

This structure was then used as the starting point for the Rietveld refinement of the neutron diffraction data. The refinement was performed using the GSAS-II programme and constraints were initially placed upon the carbonate group within the system which included O–C–O angles constrained to 120° and C–O bond lengths constrained to 1.28 Å, in line with those expected for carbonate. In line with expectations that oxygen vacancies would be less favourable around the Yb site, the carbonate group was shown to be orientated with two of its oxygens directed towards the Yb sites, with the remaining oxygen equatorial to the carbonate layer. This gives an essentially square pyramidal Yb with a sixth longer bond to the carbonate oxygen.

There was no evidence for superlattice reflections/lowering of symmetry indicative of ordering of the orientation of the carbonate groups. In the final Rietveld refinement of the $Ba_3Yb_2O_5CO_3$ structure, the constraints on the O–C–O angles and C–O distances were removed (the only constraint included was that the sum of the occupancies of these O sites equal 3 in line with requirements for a carbonate group). This refinement led to a good fit to the data with the structural parameters and bond distances given in Tables 1 and 2, and the observed,

Table 1 Structural parameters for $Ba_3Yb_2O_5CO_3$

Atom	*x*	*y*	*z*	Site occupancy	Wyckoff position	U_{iso}
C1	0.5	0.435(2)	0.5	0.250	4o	0.009(1)
Ba1	0.0	0.0	0.0	1.000	1a	[a]
Ba2	0.0	0.0	0.3358(6)	1.000	2g	[a]
Yb1	0.5	0.5	0.1773(2)	1.000	2h	0.018(1)
O1	0.0	0.5	0.1995(3)	1.000	4i	[a]
O2	0.5	0.5	0.0	1.000	1c	[a]
O3	0.5	0.148(3)	0.5	0.210(14)	4o	[a]
O4	0.397(2)	0.5	0.4019(9)	0.270(7)	8t	[a]

Atom	U_{11}	U_{22}	U_{33}	U_{12}	U_{13}	U_{23}
Ba1	0.034(1)	0.034(1)	0.015(3)	0.000	0.000	0.000
Ba2	0.024(1)	0.024(1)	0.030(2)	0.000	0.000	0.000
O1	0.008(1)	0.026(1)	0.071(1)	0.000	0.000	0.000
O2	0.088(1)	0.088(1)	0.004(2)	0.000	0.000	0.000
O3	0.020(5)	0.020(5)	0.008(5)	0.000	0.000	0.000
O4	0.043(2)	0.052(2)	0.052(2)	0.000	−0.013(1)	0.000

R_{wp} = 2.93% GOF = 1.71 *P4/mmm* *a* = 4.3258(2) Å, *c* = 11.9036(5) Å.
[a] Anisotropic atomic displacement parameters.

Table 2 Selected interatomic distances for $Ba_3Yb_2O_5CO_3$

Bond	Bond length/Å	Bond	Bond length/Å
C1–O3	1.242(16) (×1)	Ba2–O3	2.985(5) (×2)[a]
C1–O4	1.376(10) (×2)	Ba2–O4	2.871(7) (×4)[a]
Ba1–O1	3.212(2) (×8)	Yb1–O1	2.179(1) (×4)
Ba1–O2	3.059(0) (×4)	Yb1–O2	2.110(3) (×1)
Ba2–O1	2.704(5) (×4)	Yb1–O4	2.711(11) (×1)

[a] Dependent on orientation of carbonate gp.

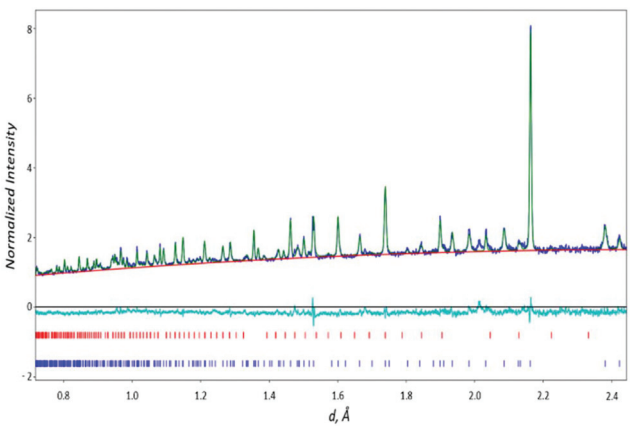

Fig. 2 Observed, calculated and difference profiles for $Ba_3Yb_2O_5CO_3$ neutron data (upper tick marks – Yb_2O_3, lower tick marks $Ba_3Yb_2O_5CO_3$).

calculated and difference neutron profiles shown in Fig. 2 (the data indicated a small amount (2.5 wt%) of Yb_2O_3 impurity, which was included in the final refinement). Given the presence of small Yb_2O_3 impurity, attempts were also made to refine the Yb site occupancy. This gave a value just above 1, and so in the final refinement was fixed at 1.0. This precludes both the presence of Yb vacancies or Ba on the Yb site (Ba has a significantly lower neutron scattering factor than Yb). The presence of this Yb_2O_3 impurity is most likely due to a small amount of amorphous $BaCO_3$, or Ba volatility as has been observed for other Ba containing perovskite systems.[31–33]

Raman studies of the $Ba_3Yb_2O_5CO_3$ material (Fig. 4) confirmed the presence of carbonate bands, with the most significant band (ν_1 symmetric stretch) seen at 1054.51 cm^{-1}. In comparison, $BaCO_3$ was also analysed with the carbonate ν_1 symmetric stretch observed at a higher energy of 1059.53 cm^{-1}. This difference confirms that the CO_3^{2-} peak was due to the $Ba_3Yb_2O_5CO_3$ material and not just small amounts of $BaCO_3$ reagent.

The final structural model is shown in Fig. 3, which shows that the structure, consists of double Yb–O layers separated by carbonate layers, representing a new example of an ordered

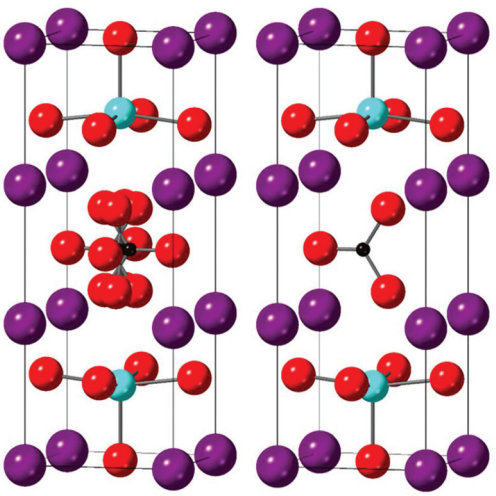

Fig. 3 (a) Refined structure of $Ba_3Yb_2O_5CO_3$ showing the split carbonate group positions attributed to local differences in carbonate orientation (b) structure illustrating a single carbonate orientation to illustrate clearer the bonding around the Yb and carbonate.

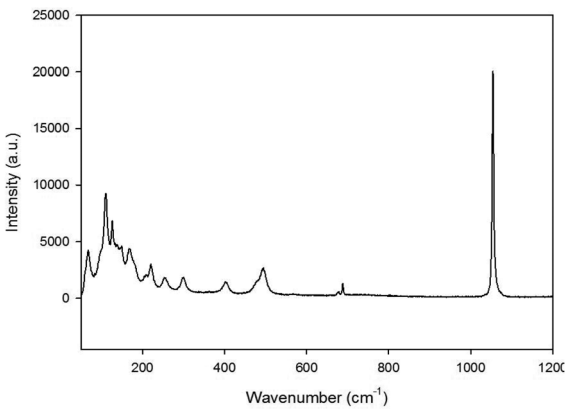

Fig. 4 Raman data for $Ba_3Yb_2O_5CO_3$.

perovskite stabilised through carbonate incorporation. The anisotropic atomic displacement parameters for O1 and O2 suggest local tilting of the YbO_6 octahedra to coincide with the adjacent carbonate orientation.

Synthesis of other $Ba_3Ln_2O_5CO_3$ (Ln = rare earth) phases

Following the successful synthesis and structure determination of $Ba_3Yb_2O_5CO_3$, the possible synthesis of analogous phases with different rare earths was investigated. Similar synthesis in air led to the successful formation of $Ba_3Ln_2O_5CO_3$ for Ln = Lu, Tm. For other rare earths (Ln = Y, Er, Ho and Dy) air synthesis led to samples with large $Ba_3Ln_4O_9$ or $BaLn_2O_4$ impurities. For these systems, better quality samples could be prepared by utilising the dry N_2 synthesis approach to limit loss of CO_2, and hence maintain the presence of carbonate in the sample. Attempts to prepare these phases for larger rare earths, *e.g.* Sm, Nd, resulted in no presence of the perovskite oxide carbonate phase. The structure obtained for $Ba_3Yb_2O_5CO_3$ was used for preliminary structure refinement to obtain cell parameters for these $Ba_3Ln_2O_5CO_3$ systems. Each refinement showed a good fit to the data. However, through the refinements it became apparent that each still contained small amounts (~3–4 wt%) of their respective Ln_2O_3 starting materials.

Table 3 Unit cell parameters for $Ba_3Ln_2O_5CO_3$ (Ln = Lu, Yb, Tm. Er, Y, Ho, Dy)

Formula	Ionic radius of Ln^{3+} (6 coordinate)[37]	Unit cell parameters		Unit cell volume
		(*a*)	(*c*)	
$Ba_3Lu_2O_5CO_3$	0.861 Å	4.3223(1) Å	11.8311(4) Å	221.03(1) Å^3
$Ba_3Yb_2O_5CO_3$	0.868 Å	4.3258(2) Å	11.9036(5) Å	222.75(2) Å^3
$Ba_3Tm_2O_5CO_3$	0.880 Å	4.3439(1) Å	11.8795(4) Å	224.16(2) Å^3
$Ba_3Er_2O_5CO_3$	0.890 Å	4.3671(3) Å	11.8623(7) Å	226.24(4) Å^3
$Ba_3Y_2O_5CO_3$	0.900 Å	4.3809(3) Å	11.8514(7) Å	227.46(4) Å^3
$Ba_3Ho_2O_5CO_3$	0.901 Å	4.3813(2) Å	11.8871(4) Å	228.19(2) Å^3
$Ba_3Dy_2O_5CO_3$	0.912 Å	4.3900(3) Å	11.9244(8) Å	229.81(4) Å^3

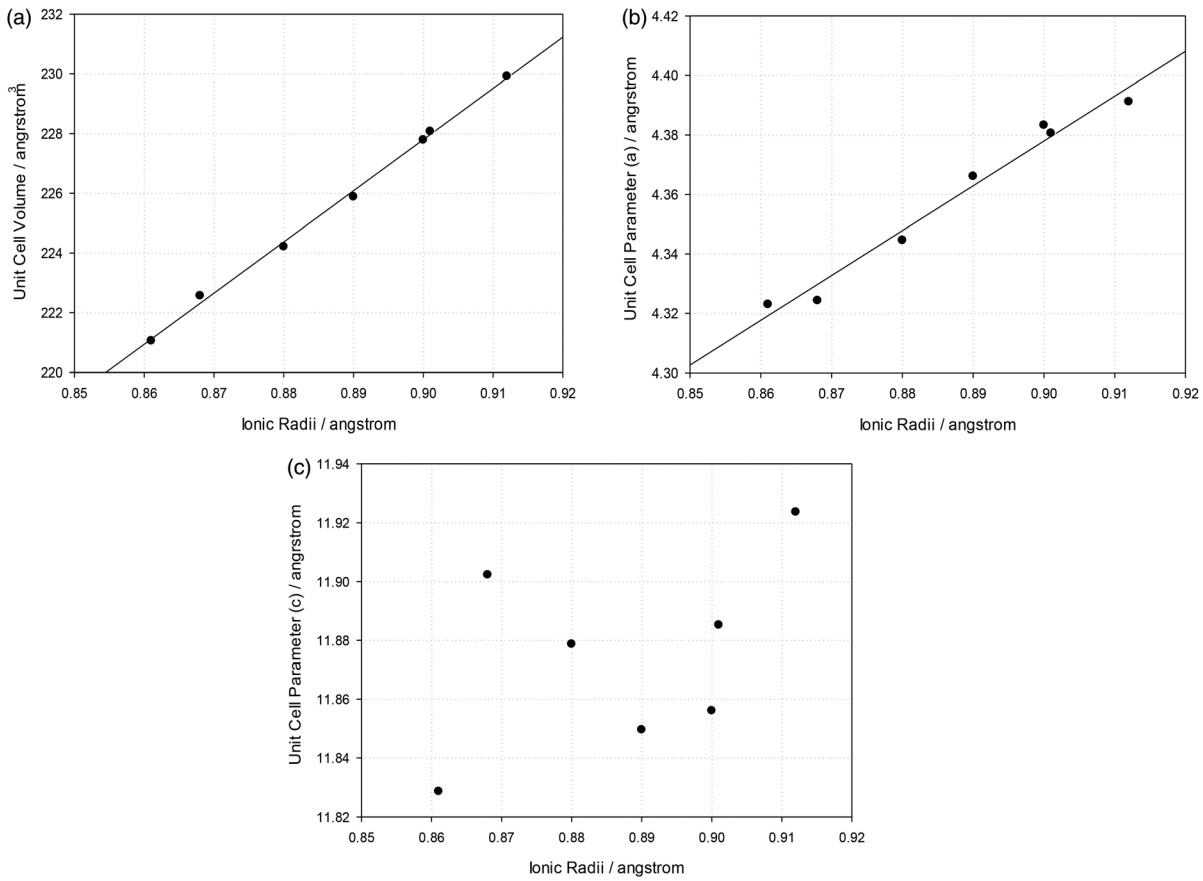

Fig. 5 (a) Variation in cell volume with Ln^{3+} ionic radius. (b) Variation in *a* cell length with Ln^{3+} ionic radius. (c) Variation in *c* cell length with Ln^{3+} ionic radius showing no systematic variation.

The refined unit cell parameters are given in Table 3, with observed, calculated and difference profile fits shown in ESI.† As expected, there is a linear increase in unit cell volume with increasing rare earth size (Table 3, Fig. 5a). However, the variation in the individual cell parameters follow a less systematic trend. While the *a* parameter shows a similar general increase with rare earth size (Fig. 5b), *c* follows a non-systematic variation (Fig. 5c). More detailed neutron diffraction structure determination would be required to explain this, which may be related to changes in local carbonate orientations. For example, it is possible that there might be some carbonate groups rotated 90° so that two oxygens are in the equatorial positions.

Conclusions

In this work, we illustrate the formation of perovskite oxide carbonate phases in the $BaCO_3 : Ln_2O_3$ phase diagram for a ratio of 3 : 1. These $Ba_3Ln_2O_5CO_3$ phases are shown to be new layered perovskites, with double Ln–O layers separated by carbonate layers, the first example of a material with such a structure. The results highlight the need to consider the potential incorporation of carbonate in perovskite materials prepared at temperatures ≤1000 °C. Thus it raises questions whether many perovskite systems prepared at low temperature (*e.g. via* sol–gel routes) may contain carbonate, affecting properties rather than simply previously considered morphological effects.

Conflicts of interest

There are no conflicts to declare.

Acknowledgements

We would like to express thanks to the Leverhulme Trust (RPG-2017-011), and Bolashak International Scholarship (PhD scholarship for Ivan Trussov) for funding. We would also like to thank the STFC ISIS Facility for the provision of neutron diffraction time. The raw neutron diffraction data file can be found in ref. 38 (within files beginning hrp68277).

Notes and references

1 C. Greaves and P. R. Slater, *J. Mater. Chem.*, 1991, **1**, 17.
2 C. Greaves and P. R. Slater, *Phys. C*, 1991, **175**, 172.
3 P. R. Slater, C. Greaves, M. Slaski and C. M. Muirhead, *Phys. C*, 1993, **208**, 193.
4 Y. Miyazaki, H. Yamane, N. Ohnishi, T. Kajitani, K. Hiraga, Y. Mori, S. Funahashi and T. Hirai, *Phys. C*, 1992, **198**, 7.
5 A. Maignan, M. Hervieu, C. Michel and B. Raveau, *Phys. C*, 1993, **208**, 116.
6 K. Kinochita and T. Yamada, *Nature*, 1992, **357**, 313.
7 M. G. Francesconi and C. Greaves, *Supercond. Sci. Technol.*, 1997, **10**, A29.
8 M. Uehara, H. Nakata and J. Akimitsu, *Phys. C*, 1993, **216**, 453.
9 R. Li, R. K. Kremer and J. Maier, *J. Solid State Chem.*, 1993, **105**, 609.
10 Y. Miyazaki, H. Yamane, T. Kajitani, N. Kobayashi, K. Hiraga, Y. Morii, S. Funahashi and T. Hirai, *Phys. C*, 1994, **230**, 89.
11 J. Akimitsu, M. Uehara, M. Ogawa, H. Nakata, K. Tomimoto, Y. Miyazaki, H. Yamane, T. Hirai, K. Kinoshita and Y. Matsui, *Phys. C*, 1992, **201**, 320.
12 B. Domenges, M. Hervieu and B. Raveau, *Phys. C*, 1993, **207**, 65.
13 Y. Shimakawa, J. D. Jorgensen, D. G. Hinks, H. Shaked and R. L. Hitterman, *Phys. Rev. B: Condens. Matter Mater. Phys.*, 1994, **50**, 16008.
14 C. A. Hancock, J. M. Porras-Vazquez, P. A. Keenan and P. R. Slater, *Dalton Trans.*, 2015, **44**, 10559.
15 V. Caignaert, B. Domenges and B. Raveau, *J. Solid State Chem.*, 1995, **120**, 279.
16 D. Pelloquin, M. Hervieu, C. Michel, N. Nguyen and B. Raveau, *J. Solid State Chem.*, 1997, **134**, 395.
17 M. Hervieu, C. Michel, D. Pelloquin, A. Maignan and B. Raveau, *J. Solid State Chem.*, 2000, **149**, 226.
18 Y. Breard, C. Michel, M. Hervieu, N. Nguyen, A. Ducouret, V. Hardy, A. Maignan, B. Raveau, F. Bouree and G. Andre, *Chem. Mater.*, 2004, **16**, 2895–2905.
19 B. Raveau, M. Hervieu, D. Pelloquin, C. Michel and R. Retoux, *Z. Anorg. Allg. Chem.*, 2005, **631**, 1831.
20 J. F. Shin, L. Hussey, A. Orera and P. R. Slater, *Chem. Commun.*, 2010, **46**, 4613.
21 J. F. Shin, D. C. Apperley and P. R. Slater, *Chem. Mater.*, 2010, **22**, 5945.
22 J. F. Shin and P. R. Slater, *J. Power Sources*, 2011, **196**, 8539.
23 C. A. Hancock, R. C. T. Slade, J. R. Varcoe and P. R. Slater, *J. Solid State Chem.*, 2011, **184**, 2972.
24 J. M. Porras-Vazquez and P. R. Slater, *J. Power Sources*, 2012, **209**, 180.
25 J. M. Porras-Vazquez, T. F. Kemp, J. V. Hanna and P. R. Slater, *J. Mater. Chem.*, 2012, **22**, 8287.
26 J. M. Porras-Vazquez and P. R. Slater, *Fuel Cells*, 2012, **12**, 1056.
27 C. A. Hancock and P. R. Slater, *Dalton Trans.*, 2011, **40**, 5599.
28 J. M. Porras-Vazquez, E. R. Losilla, P. J. Keenan, C. A. Hancock, T. F. Kemp, J. V. Hanna and P. R. Slater, *Dalton Trans.*, 2013, **42**, 5421.
29 J. M. Porras-Vazquez, T. Pike, C. A. Hancock, J. F. Marco, F. J. Berry and P. R. Slater, *J. Mater. Chem. A*, 2013, **1**, 11834.
30 J. M. Porras-Vazquez, R. I. Smith and P. R. Slater, *J. Solid State Chem.*, 2014, **1**, 132.
31 J. F. Shin, K. Joubel, D. C. Apperley and P. R. Slater, *Dalton Trans.*, 2012, **41**, 261–266.
32 J. F. Shin, A. Orera, D. C. Apperley and P. R. Slater, *J. Mater. Chem.*, 2011, **21**, 874.

33 A. D. Smith and P. R. Slater, *Inorganics*, 2014, **2**, 16.
34 J. Li, A. E. Smith, P. Jiang, J. K. Stalick, A. W. Sleight and M. A. Subramanian, *Inorg. Chem.*, 2015, **54**, 837.
35 A. J. McSloy, I. Trussov, A. Jarvis, D. J. Cooke, P. R. Slater and P. M. Panchmatia;, *J. Phys. Chem. C*, 2018, **122**, 1061.
36 B. H. Toby and R. B. Von Dreele, *J. Appl. Crystallogr.*, 2013, **46**, 544.
37 R. D. Shannon, *Acta Crystallogr., Sect. A: Cryst. Phys., Diffr., Theor. Gen. Crystallogr.*, 1976, **A32**, 751.
38 A. Gibbs, *et al.*, STFC ISIS Facility, 2017, 1720038, DOI:DOI: 10.5286/ISIS.E.87846860.